JB&JS OPEN ACCESS

A Lateral Fracture Line Affects Femoral Trochanteric Fracture Instability and Swing Motion of the Intramedullary Nail

A Biomechanical Study

Takuya Usami, MD, PhD, Naoya Takada, MD, PhD, Weerachai Kosuwon, MD, Permsak Paholpak, MD, Masami Tokunaga, MD, Hidetoshi Iwata, MD, PhD, Yusuke Hattori, MD, Yuko Nagaya, MD, PhD, Hideki Murakami, MD, PhD, and Gen Kuroyanagi, MD, PhD

Investigation performed at JFE Techno-Research, Kawasaki, Chiba, Japan

Background: An unstable trochanteric femoral fracture is a serious injury, with a 1-year mortality rate of 5.4% to 24.9%, for which there is currently no standard treatment method. The lag screw insertion site is one of the primary contact areas between the cortical bone and an intramedullary nail. We hypothesized that a posterolateral fracture causes intramedullary nail instability when the posterolateral fracture line interferes with lag screw insertion. The purpose of the present study was to investigate the effect of posterolateral fracture line morphology on intramedullary nail stability by simulating unstable trochanteric femoral fractures with a posterolateral fracture fragment.

Methods: Eighteen custom-made synthetic osteoporotic bone samples were used in the present study. Nine samples had a posterolateral fracture line interfering with the lag screw insertion hole (Fracture A), and the other 9 had a fracture line 10 mm away from the hole (Fracture B). Cyclic loading (750 N) was applied to the femoral head 1,500 times. Movement of the end cap attached to the intramedullary nail was recorded. The amplitudes of motion in the coronal plane (coronal swing motion), sagittal plane (sagittal swing motion), and axial plane (total swing motion) were evaluated. The change in the neck-shaft angle was evaluated on photographs that were made before and after the test. Medial cortical displacement was measured before and after the test.

Results: Two Fracture-A samples were excluded because the amplitude of sagittal swing motion was too large. The mean values for coronal, sagittal, and total swing motion were 1.13 ± 0.28 mm and 0.51 ± 0.09 mm ($p < 0.001$), 0.50 ± 0.12 mm and 0.46 ± 0.09 mm ($p = 0.46$), and 1.24 ± 0.24 mm and 0.69 ± 0.11 mm ($p < 0.001$) for Fractures A and B, respectively. The mean neck-shaft angle change was −8.29° ± 2.69° and −3.56° ± 2.35° for Fractures A and B, respectively ($p = 0.002$). The mean displacement of the medial cortex was 0.38 ± 1.12 mm and 0.12 ± 0.37 mm for Fractures A and B, respectively ($p = 0.57$).

Conclusions: This study showed that an unstable trochanteric femoral fracture with a posterolateral fracture line that interferes with the lag screw insertion holes is a risk factor for increased intramedullary nail instability.

An unstable trochanteric femoral fracture is a serious injury, with a high mortality rate of 5.4% to 24.9% within 1 year postoperatively[1,2]. Some poor postoperative outcomes may be explained by the etiology of the injury, including the presence of a lesser trochanteric fragment, severe osteoporosis, a reverse oblique trochanteric femoral fracture line, and a posterolateral fragment[3-7]. Recently, various options have been developed for the treatment of unstable trochanteric femoral fractures. We previously reported on the efficacy of lesser trochanteric banding for the treatment of displaced lesser

Disclosure: This study was funded by Teijin Nakashima Medical Co., Ltd. (the manufacturer of the intramedullary nails used in the study), and also partly supported by a Grant-in-Aid for Scientific Research (19K18471) from the Ministry of Education, Culture, Sports, Science, and Technology of Japan, and a Grant-in-Aid for Research (2213035) from Nagoya City University. The Article Processing Charge for open access publication was funded by Teijin Nakashima Medical Co., Ltd. The **Disclosure of Potential Conflicts of Interest** forms are provided with the online version of the article (http://links.lww.com/JBJSOA/A601).

trochanteric fragments[8]. We also reported on the use of hydroxyapatite augments to increase the screw insertion torque for the treatment of trochanteric femoral fractures[9]. However, the optimum treatment strategy for unstable trochanteric femoral fractures has not yet been established.

Li et al. reported that 33% of trochanteric femoral fractures present with a fracture line in the posterolateral aspect of the greater trochanter of the femur[10]. Furthermore, recent studies have shown that posterolateral fracture lines of trochanteric femoral fractures cause posterolateral instability[11-14]. Kim et al. and Suzuki et al. reported that the presence of a posterolateral fracture increases the risk of postoperative fragment displacement, resulting in a higher rate of implant failure and/or nonunion[3,15]. However, the etiology of instability associated with a posterolateral fracture morphology remains unclear.

We hypothesized that a posterolateral fracture would cause intramedullary nail instability when the posterolateral fracture line interferes with lag screw insertion, because the site of lag screw insertion is one of the primary contact areas between the cortical bone and the implant. In the present biomechanical study, we evaluated whether a posterolateral fracture line interfering with lag screw insertion would lead to intramedullary nail instability in synthetic bone samples with trochanteric femoral fractures. When treating more unstable fracture patterns in which the posterolateral wall fracture line interferes with the lag screw insertion hole, the orthopaedic surgeon should consider the possibility of intramedullary nail fixation becoming unstable and should consider using a longer and/or thicker intramedullary nail as one of the treatment options.

Materials and Methods

Sample Preparation

Custom-made synthetic osteoporotic bone samples that were designed with use of previously created computed tomography (CT) images of human hips (Tanac) were used in this study. These samples had a neck-shaft angle of 135°, anteversion of 25.8°, cancellous bone density of 7.5 pounds per cubic foot (pcf) (0.115 g/cm^3), cortical bone density of 60 pcf (0.92 g/cm^3), and a canal flare index (CFI) of 2.29. Two types of fracture lines were created. Fracture A consisted of a posterolateral wall comminution model in which the posterolateral wall fracture line interfered with the lag screw insertion hole. Fracture B was characterized by an intact posterolateral wall model with the fracture line 10 mm away from the lag screw insertion hole. Fractures A and B both consisted of 4-part comminuted trochanteric fractures with the same design, except for the posterolateral wall fracture line (Fig. 1). All fracture lines were cut with use of dedicated external jigs. Eighteen samples (9 samples each for Fractures A and B) were prepared for this biomechanical study. Optical Locking Solution (OLS) I intramedullary nails (diameter, 10 mm; neck angle, 125°; length, 170 mm) and OLS I lag screws (diameter,10.8 mm; length, 100 mm) (Teijin Nakashima Medical) were inserted without reaming in all samples; the lag screw tip-apex distance was 20 mm[16].

Test Protocol

All samples were fixed on a biomechanical testing machine (ElectroPuls E3000; Instron), 10° laterally from the gravitational line in the frontal plane and 12° posteriorly from the gravitational line in the sagittal plane. Cyclic vertical loads were applied to the femoral head, with a maximum load of 750 N

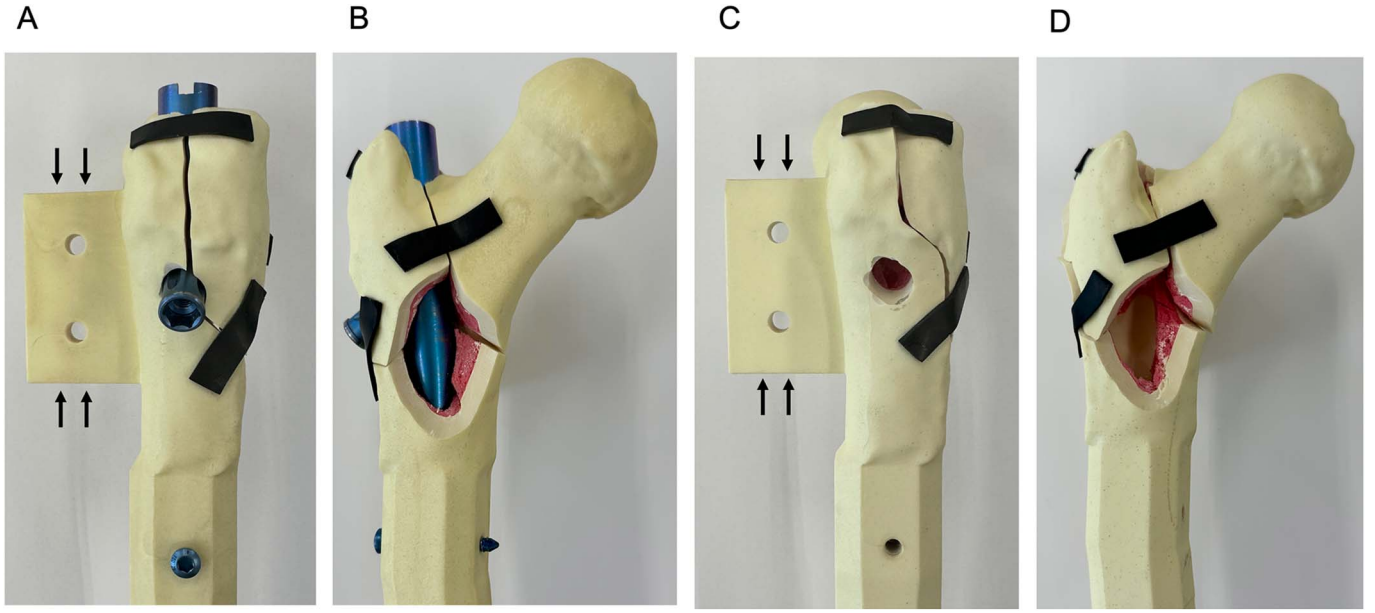

Fig. 1

Figs. 1-A through 1-D Overview of the specimens. Both fractures were 4-part comminuted trochanteric femoral fractures. Fracture A involved a lateral wall fracture line that interfered with the lag screw insertion hole (**Figs. 1-A and 1-B**). Fracture B involved a lateral wall fracture line 10 mm from the lag screw insertion hole (**Figs. 1-C and 1-D**). The structures indicated by the black arrows in Figures 1-A and 1-C were used to fix the depth gauges.

JBJS Open Access • 2024:e23.00118.

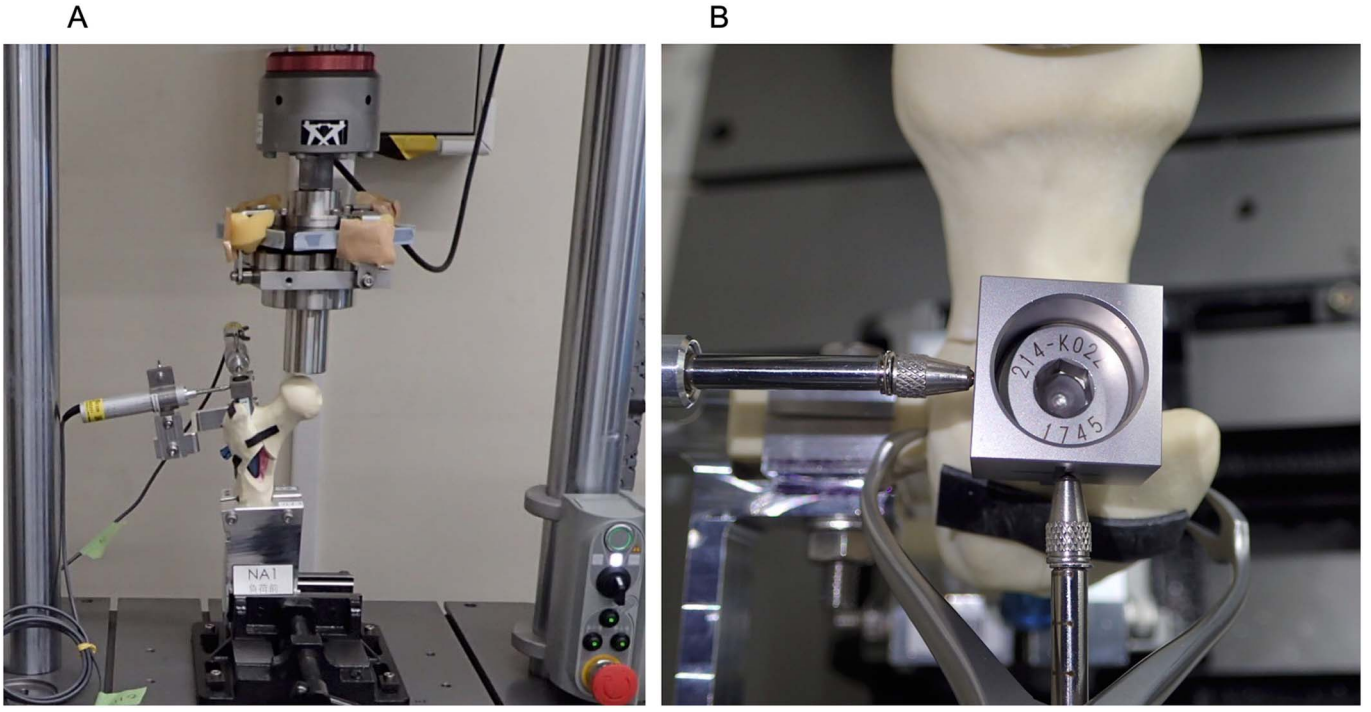

Fig. 2

Figs. 2-A and 2-B Photographs showing a specimen in the biomechanical testing machine. The specimen was placed on the machine 10° laterally from the gravitational line in the frontal plane and 12° posteriorly from the gravitational line in the sagittal plane with use of a clamp. We calculated the movement of the block attached to the top of the intramurally nail. The movement of the block was captured with digital depth gauges that were fixed perpendicularly to each other.

and a minimum load of 75 N, at 3 Hz. The tests ended after 1,500 loading cycles (Fig. 2).

Data Assessments

The movement of the intramedullary nails was measured with use of 2 digital depth gauges (DTH-A30; Kyowa Electronic Instruments); 1 gauge was fixed parallel to the femoral neck, and the other was fixed perpendicular to the femoral neck. Intramedullary nail instability was evaluated by recording the movement of the dedicated end cap with use of depth gauges that were fixed to the proximal anterior cortex (Fig. 3). The movement was termed the "swing motion" of the intramedullary nails. The amount of coronal swing motion was defined as the amplitude of the depth gauge in the coronal (mediolateral)

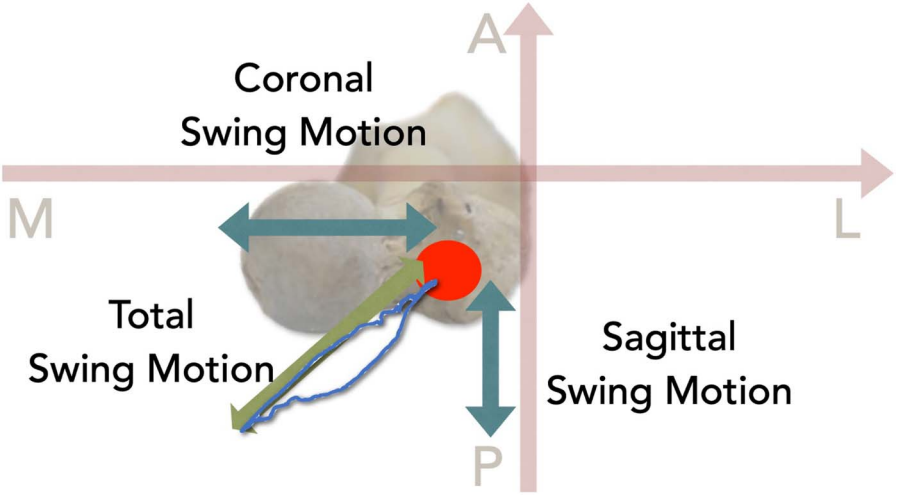

Fig. 3

Illustration showing the axis and the swing motion; the axis was set perpendicularly in relation to the femoral neck. A = anterior, M = medial, P = posterior, L = lateral.

JBJS Open Access • 2024:e23.00118. **openaccess.jbjs.org** 4

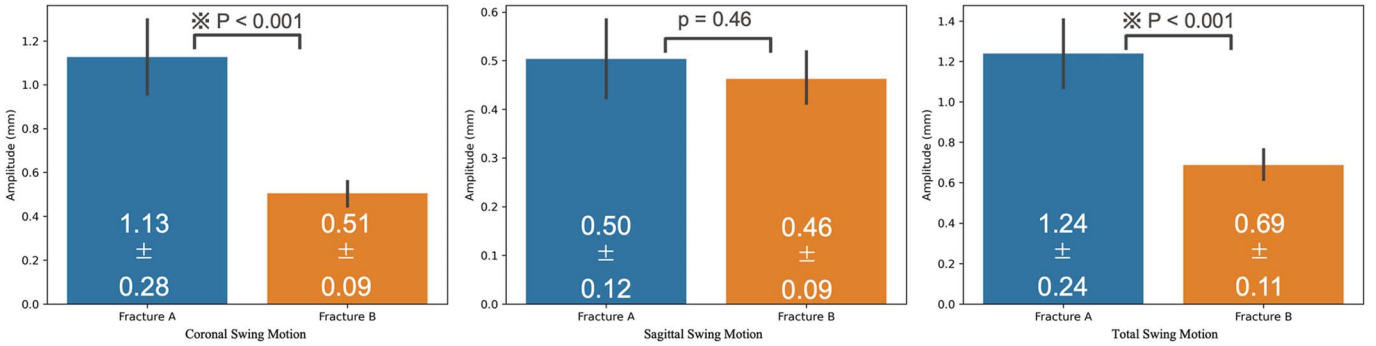

Fig. 4

Bar graphs summarizing sagittal swing motion, coronal swing motion, and total swing motion in Fractures A and B. Fracture A had significantly greater coronal swing motion and total swing motion. The error bars represent the standard deviation .

plane, the amount of sagittal swing motion was defined as that in the sagittal (anterolateral) plane, and the amount of total swing motion was defined as the maximum amplitude in the axial plane (Fig. 4). The coronal swing motion, sagittal swing motion, and total swing motion were all analyzed during the last loading cycle. The amount of subsidence of the femoral head was measured with use of a biomechanical testing machine and was calculated at the start and end of the tests. ImageJ2 software (version 2.3.0) was used to calculate the change in the neck-shaft angle from pictures acquired before and after the test (Figs. 5-A and 5-B). Displacement of the medial cortex was measured with use of a vernier caliper before and after each test. Displacement was considered to be positive when the marked portion of the proximal bone fragment was displaced anteriorly (Fig. 5-C).

Statistical Analysis

The values were shown as mean and the standard deviation (SD). Continuous variables were compared between Fractures A and B with use of the Welch t test. The level of significance was set at $p < 0.05$. The R statistics package (version 3.5.1; R Core Team, Foundation for Statistical Computing) was used for all analyses.

Results

Two Fracture A samples (Fractures A3 and A4) were excluded from the study because the amplitudes of sagittal swing motion were too large and the depth gauge deviated from the measurement range. The other samples did not break during testing. All swing motions were detected in the posteromedial

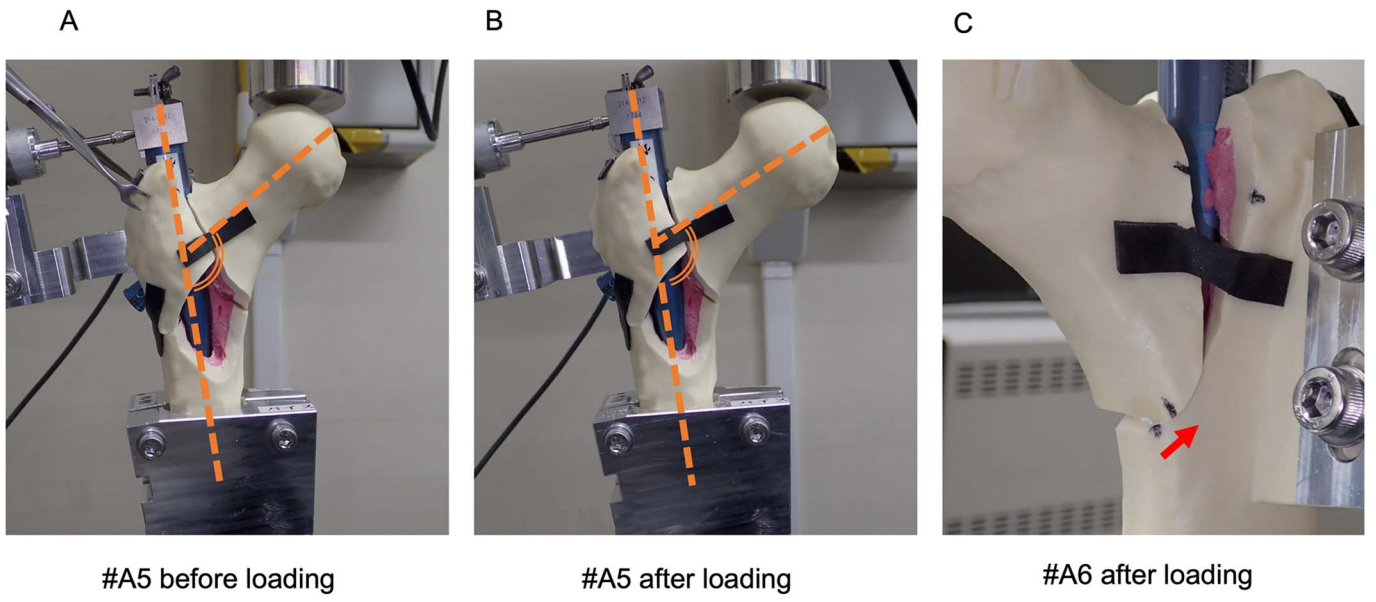

Fig. 5

Figs. 5-A, 5-B, and 5-C Varus deformities were calculated with use of ImageJ2 software. We calculated the varus angles indicated by the bold dashed lines. The varus angle after loading (**Fig. 5-B**) was smaller than that before loading (**Fig. 5-A**), as shown for a representative fracture (A5). The measured displacement between before and after loading was calculated as the displacement of the medial cortex (**Fig. 5-C**), as shown for a representative fracture (A6). The arrow shows the displacement of the medial cortex.

TABLE I Summary of Variables After Mechanical Testing

Variable*	Fracture A (N = 7)	Fracture B (N = 9)	P Value
Subsidence of femoral head *(mm)*	10.63 ± 1.97	8.76 ± 0.85	0.048†
Coronal swing motion *(mm)*	1.13 ± 0.28	0.51 ± 0.09	<0.001‡
Sagittal swing motion *(mm)*	0.50 ± 0.12	0.46 ± 0.09	0.46
Total swing motion *(mm)*	1.24 ± 0.24	0.69 ± 0.11	<0.001‡
Change in neck-shaft angle *(deg)*	−8.29 ± 2.69	−3.56 ± 2.35	0.002†
Displacement of medial cortex *(mm)*	0.38 ± 1.12	0.12 ± 0.37	0.57

*The values are given as the mean and the standard deviation. †P < 0.05. ‡P < 0.01.

direction (Fig. 4). Videos 1 and 2 demonstrate the swing motion from the front and posterolateral views, respectively. The mean coronal swing motion was 1.13 ± 0.28 mm and 0.51 ± 0.09 mm for Fractures A and B, respectively ($p < 0.001$). The mean sagittal swing motion was 0.50 ± 0.12 mm and 0.46 ± 0.09 mm for Fractures A and B, respectively ($p = 0.46$). The mean total swing motion was 1.24 ± 0.24 mm and 0.69 ± 0.11 mm for Fractures A and B, respectively ($p < 0.001$). The subsidence of the femoral head reached a plateau after approximately 1,000 cycles in all fractures. The amount of subsidence of the femoral head at the end of the tests was 10.63 ± 1.97 mm and 8.76 ± 0.85 mm for Fractures A and B, respectively ($p = 0.048$). Varus deformities were observed in all samples after the test. The mean change in the neck-shaft angle was −8.29° ± 2.69° and −3.56° ± 2.35° for Fractures A and B, respectively ($p = 0.002$). The mean displacement of the medial cortex was 0.38 ± 1.12 mm and 0.12 ± 0.37 mm for Fractures A and B, respectively ($p = 0.57$) (Table I).

Discussion

The present biomechanical study showed that the interference of the posterolateral wall fracture line with the lag screw insertion hole exacerbates the amount of subsidence of the femoral head, coronal swing motion, total swing motion, and varus deformity. Chang et al., in a clinical study, reported that coronal instability leads to instability when the fracture line includes a lag screw insertion hole[7]. Similarly, Kim et al. reported that a posterolateral fracture is a risk factor for postoperative nonunion[3]. In the present study, Fracture A showed increased coronal swing motion and subsidence of the femoral head compared with those shown by Fracture B. Furthermore, greater varus deformity of the intramedullary nails was observed in association with Fracture A compared with Fracture B.

In the present study, we found no significant difference in sagittal swing motion between Fractures A and B; however, the amount of sagittal swing motion in the cases of 2 fractures (Fractures A3 and A4) was very large, and the difference in sagittal swing motion may reach significance in further studies. Overall, these findings suggest that posterolateral wall comminution with a posterolateral fracture causes intramedullary nail instability not only in the coronal plane but also in the entire intramedullary nail. To our knowledge, this is the first biomechanical study to demonstrate the importance of posterolateral wall fracture morphology. Thus, when treating a fracture that has a posterolateral fracture line, additional treatment options, such as thicker nails, long nails, and multiple distal screw insertions, may be useful to prevent the movement of intramedullary nails. Previously, most orthopaedic surgeons used only radiographs for preoperative evaluation. As the incidence of intertrochanteric fractures is high and is predicted to increase, the use of CT scans for routine evaluation of intertrochanteric fractures will increase the burden of health-care cost and radiation to patients. Isida et al. reported that radiographic assessment underestimated the complexity of posterior and posterolateral wall fractures compared with CT images[17]. Therefore, orthopaedic surgeons should accurately assess posterior and posterolateral wall fractures with CT scans and should consider using longer and/or thicker intramedullary nails in cases of unstable fractures. Our results may encourage surgeons to further evaluate posterolateral wall fracture lines with use of CT. We choose 10-mm-diameter and 170-mm-length nails for unstable intertrochanteric fractures in this study because short femoral nails such as TFNA (diameter, 10 mm; length, 170 mm) (DePuy Synthes) and InterTAN (diameter, 10 mm; length, 180 mm) (Smith & Nephew) were used for experiments involving unstable fracture models[18]. As our results showed a large amount of swing motion in group A, surgeons should consider using a longer and/or thicker intramedullary nail for fractures where the fracture line interferes with the lag screw insertion hole.

Regarding the osteoporotic condition of the custom-made synthetic bone used in the present study, our samples had a CFI of 2.29, categorized as a stove pipe, which is commonly observed in patients with severe osteoporosis[19]. A previous micro-CT analysis involving elderly patients showed that the trabecular and cortical bone mineral densities of the femoral head were 0.064 g/cm^3 and 0.69 g/cm^3, respectively, at a mean age of 93 years and 0.22 g/cm^3 and 0.96 g/cm^3, respectively, at a mean age of 76 years[20]. The custom-made synthetic bone used in the present study had a density of 7.5 pcf for cancellous bone and 60 pcf for cortical bone, corresponding to 0.115 g/cm^3 and 0.92 g/cm^3, respectively[20]. Therefore, this synthetic bone was within the osteoporotic bone range. The custom-made synthetic bone samples were designed with use of previously created CT images of human hips. The

neck-shaft angle of 135° in our bone model was within the normal range, but the anteversion of the femoral neck of 25.8° (which was calculated between the femoral neck axis and the posterior epicondyle axis) was greater than that in a normal femur (10.4° ± 6.7°)[21]. In the present study, we used only the proximal part of the femur. Thus, in our bone model, we measured both the supra-trochanteric and infra-trochanteric torsion angles, which were determined on the basis of the positions of the lesser trochanter and the femoral neck axis, and found that the angle between them was 39.8°, which was within the range of 37° ± 8.7° in healthy people[22]. Thus, our bone samples appear to be equivalent to the normal and average proximal femoral anatomy.

The test protocol was designed to mimic a normal gait cycle. The International Organization for Standardization (ISO) proposed that the angle during biomechanical testing should be 7° posterior and 10° lateral in the sagittal and coronal planes, respectively. Previous studies have demonstrated that after total hip arthroplasty (THA), the femoral head is loaded with up to 50% of the body weight in the posterior direction during the gait cycle[23,24]. The samples in the present study were oriented 12° posteriorly to yield a posterior vector force equal to 50% of the loading force. In contrast, the force component has been reported to be directed 13° to 21° laterally in the coronal plane[23]. Therefore, our biomechanical testing protocol was consistent with the ISO and normal gait cycles.

The present study had several limitations. First, all experiments were solely performed on low-density synthetic bone tissue. O'Neill et al. reported that synthetic bone with a density of 0.08 g/cm^3 did not represent cadaveric bone because osteoporotic synthetic bone did not show similar force-displacement curves or peak force during a pushout study[25]. To minimize this disparity, we used a loading force of 750 N, which corresponds to the load in a normal gait, and found that the subsidence of the femoral head was sufficiently small in all cases. Further studies involving fresh-frozen cadaveric specimens are needed to simulate the human environment. Second, posterolateral fractures may be displaced by the forces of the lateral rotator muscles, but the present study did not simulate bone-muscle interactions.

In conclusion, our study showed that a posterolateral fracture that interferes with lag screw insertion holes could be an independent risk factor for increased instability of intramedullary nails. Further surgical strategies aimed at minimizing the coronal swing motion, total swing motion, and changes in the neck-shaft angle are necessary to determine the best treatment strategies for unstable femoral trochanteric fractures. ■

Note: The authors thank Mr. J. Fukumoto, of Teijin Nakashima Medical Co., Ltd., for technical assistance with the experiments. He did not give us any writing assistance.

Takuya Usami, MD, PhD[1,2]
Naoya Takada, MD, PhD[3]
Weerachai Kosuwon, MD[4]
Permsak Paholpak, MD[4]
Masami Tokunaga, MD[5]
Hidetoshi Iwata, MD, PhD[3]
Yusuke Hattori, MD[1,2]
Yuko Nagaya, MD, PhD[2]
Hideki Murakami, MD, PhD[1]
Gen Kuroyanagi, MD, PhD[1,6]

[1]Department of Orthopaedic Surgery, Nagoya City University Graduate School of Medical Sciences, Nagoya, Aichi, Japan

[2]Department of Orthopaedic Surgery, Nagoya City University East Medical Center, Nagoya, Aichi, Japan

[3]Department of Orthopaedic Surgery, Kainan Hospital, Yatomi, Aichi, Japan

[4]Department of Orthopaedics, Faculty of Medicine, Khon Kaen University, Khon Kaen, Thailand

[5]Department of Orthopaedic Surgery, Fukuoka Orthopaedic Hospital, Fukuoka, Fukuoka, Japan

[6]Department of Rehabilitation Medicine, Nagoya City University Graduate School of Medical Sciences, Nagoya, Aichi, Japan

Email for corresponding author: kokuryugen@yahoo.co.jp

References

1. McLeod K, Brodie MP, Fahey PP, Gray RA. Long-term survival of surgically treated hip fracture in an Australian regional hospital. Anaesth Intensive Care. 2005 Dec; 33(6):749-55.

2. Li XP, Zhang P, Zhu SW, Yang MH, Wu XB, Jiang XY. All-cause mortality risk in aged femoral intertrochanteric fracture patients. J Orthop Surg Res. 2021 Dec 20;16(1):727.

3. Kim KH, Kang MS, Lim EJ, Park ML, Kim JJ. Posterior Sagging After Cephalomedullary Nailing for Intertrochanteric Femur Fracture is Associated with a Separation of the Greater Trochanter. Geriatr Orthop Surg Rehabil. 2020 Aug 4;11: 2151459320946013.

4. Gleich J, Neuerburg C, Linhart C, Keppler AM, Pfeufer D, Kammerlander C, Böcker W, Ehrnthaller C. Inferior Outcome after Unstable Trochanteric Fracture Patterns Compared to Stable Fractures in the Elderly. J Clin Med. 2021 Jan 6;10(2):171.

5. Roux C, Thomas T, Paccou J, Bizouard G, Crochard A, Toth E, Lemaitre M, Maurel F, Perrin L, Tubach F. Refracture and mortality following hospitalization for severe osteoporotic fractures: The Fractos Study. JBMR Plus. 2021 May 14;5(7):e10507.

6. Haidukewych GJ, Israel TA, Berry DJ. Reverse Obliquity Fractures of the Intertrochanteric Region of the Femur. J Bone Joint Surg Am. 2001;83(5):643-50.

7. Chang SM, Hou ZY, Hu SJ, Du SC. Intertrochanteric Femur Fracture Treatment in Asia: What We Know and What the World Can Learn. Orthop Clin North Am. 2020 Apr; 51(2):189-205.

8. Usami T, Takada N, Nishida K, Sakai H, Iwata H, Sekiya I, Ueki Y, Murakami H, Kuroyanagi G. Banding with lesser trochanter fragment using nonabsorbable tape in trochanteric femoral fractures. SICOT J. 2021;7:33.

9. Iwata H, Takada N, Kuroyanagi G, Ikuta K, Usami T, Sekiya I, Murakami H. Effect of hydroxyapatite tubes on the lag screw intraoperative insertion torque for the treatment of intertrochanteric femoral fractures. Injury. 2021 Nov;52(11): 3377-81.

10. Li J, Tang S, Zhang H, Li Z, Deng W, Zhao C, Fan L, Wang G, Liu J, Yin P, Xu G, Zhang L, Tang P. Clustering of morphological fracture lines for identifying intertrochanteric fracture classification with Hausdorff distance-based K-means approach. Injury. 2019 Apr;50(4):939-49.

11. Shoda E, Kitada S, Sasaki Y, Hirase H, Niikura T, Lee SY, Sakurai A, Oe K, Sasaki T. Proposal of new classification of femoral trochanteric fracture by three-dimensional computed tomography and relationship to usual plain X-ray classification. J Orthop Surg (Hong Kong). 2017 Jan;25(1):2309499017692700.

12. Cho JW, Kent WT, Yoon YC, Kim Y, Kim H, Jha A, Durai SK, Oh JK. Fracture morphology of AO/OTA 31-A trochanteric fractures: A 3D CT study with an emphasis on coronal fragments. Injury. 2017 Feb;48(2):277-84.

13. Tan BY, Lau AC, Kwek EB. Morphology and fixation pitfalls of a highly unstable intertrochanteric fracture variant. J Orthop Surg (Hong Kong). 2015 Aug;23(2):142-5.

14. Fan J, Xu X, Zhou F, Zhang Z, Tian Y, Ji H, Guo Y, Lv Y, Yang Z, Hou G. Risk factors for implant failure of intertrochanteric fractures with lateral femoral wall fracture after intramedullary nail fixation. Injury. 2021 Nov;52(11):3397-403.
15. Suzuki N, Kijima H, Tazawa H, Tani T, Miyakoshi N. Occurrence and clinical outcome of lateral wall fractures in proximal femoral fractures whose fracture line runs from femoral basal neck to subtrochanteric area. Medicine (Baltimore). 2022 Dec 2;101(48):e32155.
16. Kane P, Vopat B, Heard W, Thakur N, Paller D, Koruprolu S, Born C. Is tip apex distance as important as we think? A biomechanical study examining optimal lag screw placement. Clin Orthop Relat Res. 2014 Aug;472(8):2492-8.
17. Isida R, Bariatinsky V, Kern G, Dereudre G, Demondion X, Chantelot C. Prospective study of the reproducibility of X-rays and CT scans for assessing trochanteric fracture comminution in the elderly: a series of 110 cases. Eur J Orthop Surg Traumatol. 2015 Oct;25(7):1165-70.
18. Pastor T, Zderic I, Gehweiler D, Gardner MJ, Stoffel K, Richards G, Knobe M, Gueorguiev B. Biomechanical analysis of recently released cephalomedullary nails for trochanteric femoral fracture fixation in a human cadaveric model. Arch Orthop Trauma Surg. 2022 Dec;142(12):3787-96.
19. Noble PC, Alexander JW, Lindahl LJ, Yew DT, Granberry WM, Tullos HS. The anatomic basis of femoral component design. Clin Orthop Relat Res. 1988 Oct;(235):148-65.
20. Whitmarsh T, Otake Y, Uemura K, Takao M, Sugano N, Sato Y. A cross-sectional study on the age-related cortical and trabecular bone changes at the femoral head in elderly female hip fracture patients. Sci Rep. 2019 Jan 22;9(1):305.
21. Reikerås O, Høiseth A, Reigstad A, Fönstelien E. Femoral neck angles: a specimen study with special regard to bilateral differences. Acta Orthop Scand. 1982 Oct;53(5):775-9.
22. Waisbrod G, Schiebel F, Beck M. Abnormal femoral antetorsion-a subtrochanteric deformity. J Hip Preserv Surg. 2017 Apr 12;4(2):153-8.
23. Bergmann G, Bender A, Dymke J, Duda G, Damm P. Standardized Loads Acting in Hip Implants. PLoS One. 2016 May 19;11(5):e0155612.
24. Hua X, Li J, Jin Z, Fisher J. The contact mechanics and occurrence of edge loading in modular metal-on-polyethylene total hip replacement during daily activities. Med Eng Phys. 2016 Jun;38(6):518-25.
25. O'Neill F, Condon F, McGloughlin T, Lenehan B, Coffey C, Walsh M. Validity of synthetic bone as a substitute for osteoporotic cadaveric femoral heads in mechanical testing: A biomechanical study. Bone Joint Res. 2012 Apr 1;1(4):50-5.